Supersonic Flow Around Rocket Fins at a High Altitude
ME 548: STAR-CCM+ Final Project

Catie Spivey

18 March 2021, Updated 13 April 2021

1. Overview

The Portland State Aerospace Society (PSAS) is an amateur rocketry group working on a liquid fueled rocket that is intended to reach an altitude of 100 km. This rocket is known as Launch Vehicle 4 (LV4) and is shown in Figure 1. While the initial design for LV4 comes from scaling up the previous launch vehicle, LV3.1, many aspects of the design are untested and may need to change due to the demands of the higher speed and altitude. LV4 is currently 24 feet long with an outer diameter of 12 inches. The design is determined by the output of the LV4 Multidisciplinary Optimization (MDO) code [1], which is updated regularly with information such as component mass and engine thrust. The goal of this project is to evaluate the coefficients of drag and lift for each fin shape, which would then be used with the MDO to determine optimal shape of the fins for the rocket. Additionally, the magnitude and location of maximum pressure on the frontal face of the fins is found as a supplement for FEA models to determine the structural feasibility of the fin can.

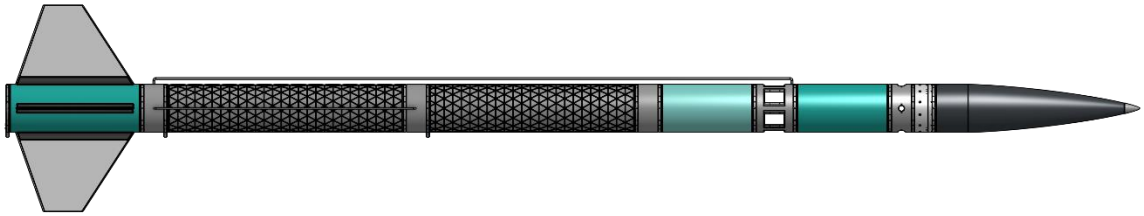

Figure 1: Version 1 (V1) of Portland State Aerospace Society's Launch Vehicle 4 (LV4) airframe.

1.1 Four Fin Shapes

The four fins under consideration have two planform shapes: trapezoid (Figure 2) and swept (Figure 3); and two cross-sectional shapes: rectangular and diamond (Figure 4). The diamond cross section is created by chamfering the front and back edges. The four shapes are abbreviated in this report as "RT," "DT," "RS," and "DS" as shown in Table 1.

Table 1: Table showing abbreviated names of the four fin shapes.

		Planform Shape	
		Trapezoid	**Swept**
Side Shape	**Rectangular**	RT	RS
	Diamond	DT	DS

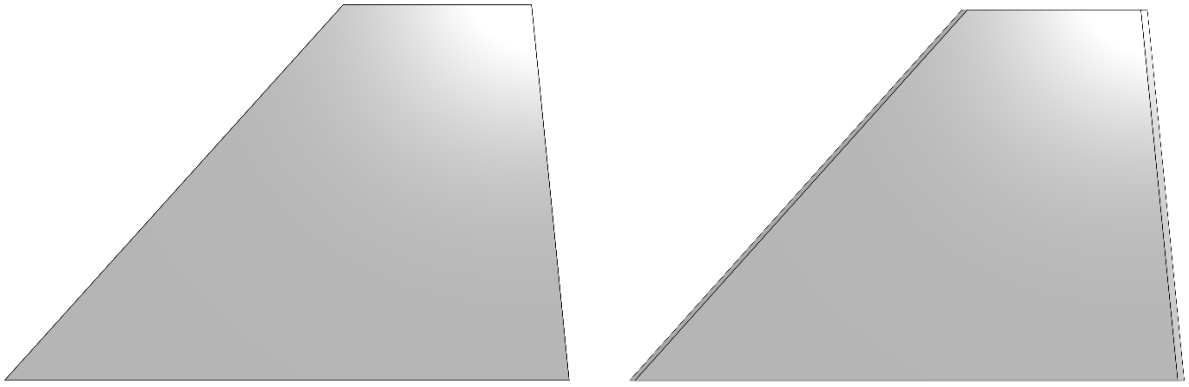

Figure 2: Trapezoidal Fins. LEFT: Rectangular cross section (RT). RIGHT: Diamond cross section (DT).

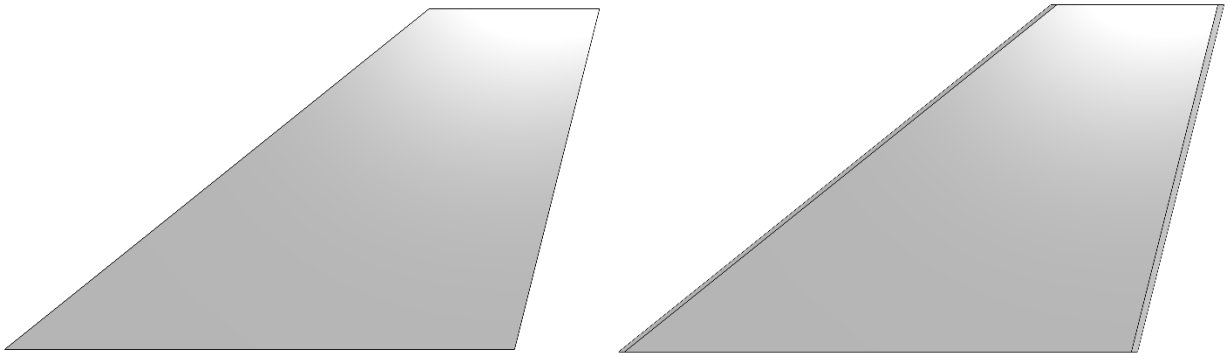

Figure 3: Swept Fins. LEFT: Rectangular cross section (RS). RIGHT: Diamond cross section (DS).

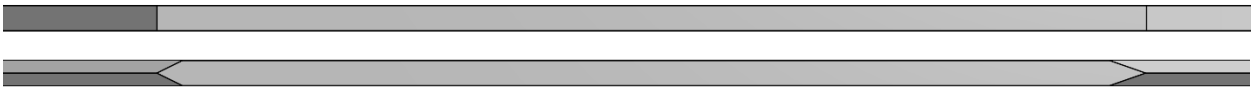

Figure 4 TOP: Top view of a rectangular fin. BOTTOM: Top view of a diamond fin (front and back edges are chamfered).

1.2 Properties of Air and Flow at Altitude

This project uses an altitude of 23,000 m and a velocity of 1300 m/s because the LV4 MDO is estimating a maximum Mach number of 4.33 to occur at this instance. Table 2 gives the values of the properties of the air flow field that will be used in this simulation:

Table 2: *Properties of air flow field at an altitude of 23,000 meters used in this simulation.*

Property	Value
Static Temperature	219.59 K
Density	0.059612 kg/m^3
Dynamic Viscosity	1.4376 x 10^{-5} Pa-s
Absolute Pressure	3741 Pa
Thermal Conductivity	0.02003895 W/m-K
Speed of Sound	300 m/s
Mach number	4.33
Velocity	1300 m/s

2. Physical Model and Boundary Conditions

A simplified geometry of the body of the rocket with a nose cone was modeled to allow for the flow to develop before it reaches the fins. An overall rocket length of 24 feet was used with an outer diameter of 12 inches. Further detail of this geometry is not relevant to the flow at the fin surface. A trapezoidal fin was modeled at the end of the rocket using the geometry seen in Figure 5. Swept fins are created using a negative Offset Trailing value, while diamond cross sections are created by chamfering the edges after extrusion. The values used in the four simulations of this project are summarized in Table 3, with all four fins having an equal planform area of 400 in^2, which is important for comparing drag and lift coefficients.

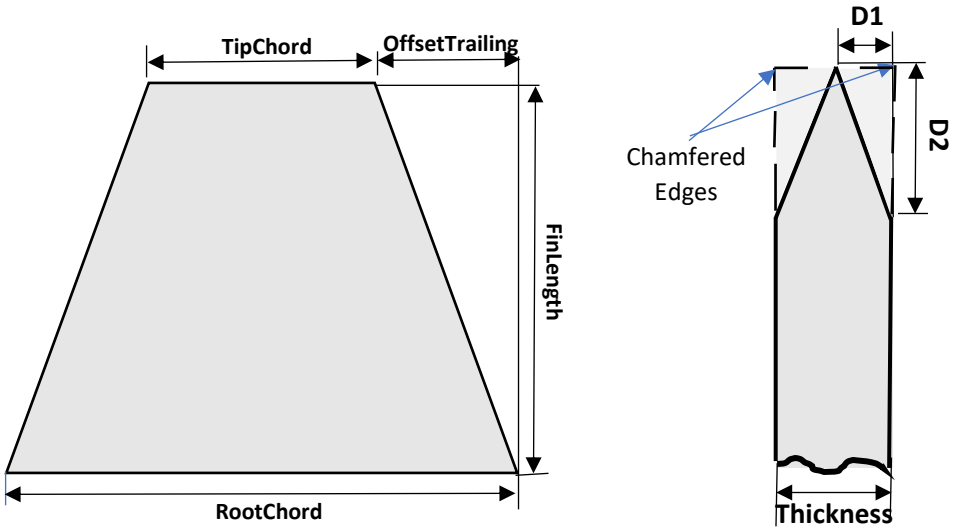

Figure 5 LEFT: Planform view of geometry of a LV4 fin. Swept fins will have a negative Offset Trailing value. RIGHT: Cross section view of geometry of a diamond fin. D1 and D2 are dimensions of the chamfered front and back edges.

Table 3: Table of values for fin geometry.

Variable	Description	Value [in]			
		RT	DT	RS	DS
RootChord	Length of bottom surface of fin	30	30	30	30
TipChord	Length of top surface of fin	10	10	10	10
OffsetTrailing	Distance from top back edge to bottom back edge	2	2	-5	-5
FinLength	Length from top surface to bottom surface of fin	20	20	20	20
Thickness	Thickness of fin	0.125	0.125	0.125	0.125
D1	Distance the chamfered edge is cut towards center line of fin	N/A	0.0625	N/A	0.0625
D2	Distance the chamfered edge is cut towards body of fin	N/A	0.56	N/A	0.56

The surrounding air flow was modeled as a cylinder with a rounded front surface and the entire geometry was cut to only ¼ of the full axisymmetric geometry, representing one of the four fins on the rocket (Figure 6). We can assume that the flow is axisymmetric about the rocket's centerline when there is no angle of attack to the flow (the rocket body, and thus the fins, are parallel to the flow). The values used in all four fin simulations are summarized in Table 4.

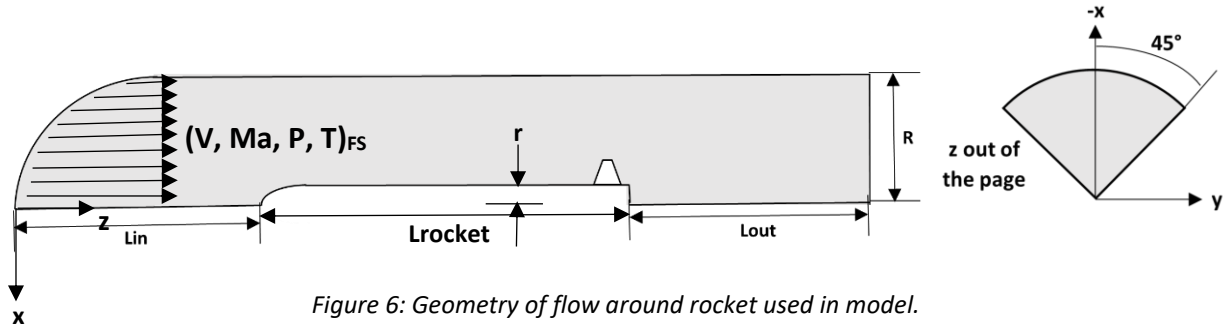

Figure 6: Geometry of flow around rocket used in model.

Table 4: Values of variables used in modeling CAD of flow geometry.

Variable	Description	Value [feet]
Lin	Distance from Free Stream start to rocket body tip	12.4
Lout	Distance from rocket body tail to Free Stream end	16.4
R	Radial distance of Free Stream cylindrical boundary	16.4
r	Radius of rocket body	0.5
Lrocket	Length of rocket body	24

Figure 7: The cylindrical surface is a boundary of type "Free Stream" and is shown in orange.

The cylindrical boundary surface seen in Figure 7 is of the type "Free Stream" [2]. Using the Mach Number + Pressure + Temperature option, the values from Table 2 were used to change Flow Direction, Mach Number, and Static Temperature. Reference Pressure was not changed because it is a gauge pressure.

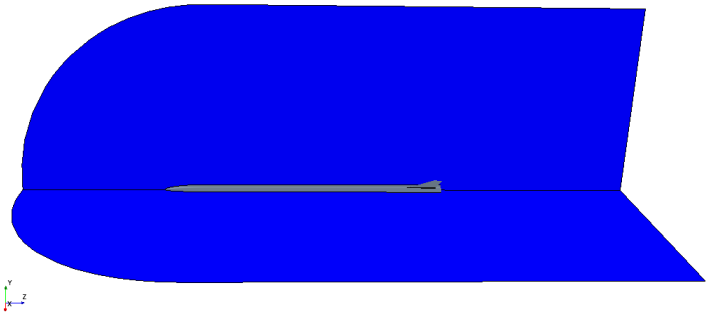

Figure 8: The two surfaces resulting from the revolved cut of the axisymmetric geometry are shown in blue and are separate boundaries, each of the type "Symmetry."

The two surfaces that result from the revolved cut of the axisymmetric geometry are two separate boundary surfaces, each of the type “Symmetry” (Figure 8).

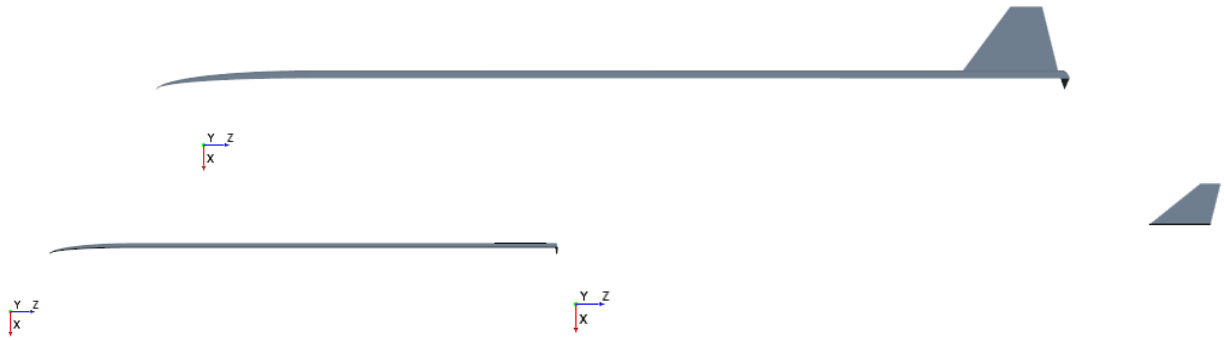

Figure 9: TOP: Full rocket body. BOTTOM: The rocket body and fin surfaces are separate and of the boundary type “Wall.”

The rocket body and fin are two separate boundary surfaces, each of the type “Wall,” allowing for analysis to happen on the fin region alone (Figure 9).

3. CFD Software Features

The following models were selected for the Physics Continuum, with Auto-select turned on to result in all models shown in Figure 10:

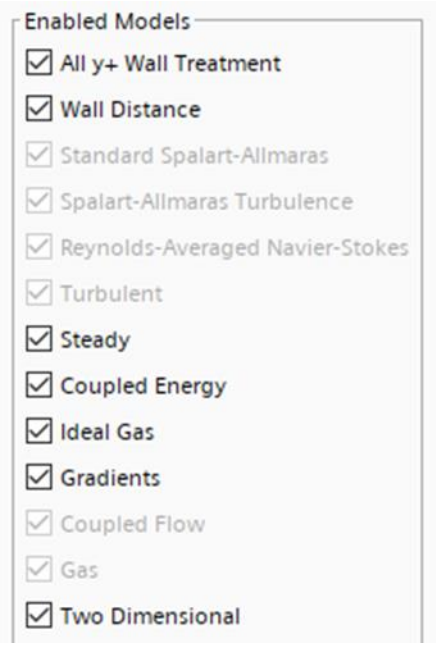

- Two-dimensional
- Gas
- Coupled Flow
- Ideal Gas
- Steady
- Turbulent
- Spalart-Allmaras Turbulence [3]

The values for the Dynamic Viscosity and Thermal Conductivity of air were changed to match Table 2, as well as the Reference Pressure, Initial Velocity, and Initial Static Temperature. The Minimum Allowable Pressure was changed to -1000 Pa to allow for negative pressures to develop behind the rocket.

Figure 10: *Enabled Models for Physics Continuum.*

4. CFD Mesh

The Automated Mesh used the following meshers: Surface Remesher, Trimmed Cell, Prism Layer. The modified values can be found in Table 5, with all others left as default.

Table 5: Automated Mesh parameters that were changed.

Control	Value
Prism Layer Distribution Mode	Wall Thickness
Prism Layer Gap Fill Percentage	45.0
Prism Layer Minimum Thickness Percentage	0.05
Prism Layer Reduction Percentage	0.0
Base Size	0.5 m
Number of Prism Layers	8
Prism Layer Near Wall Thickness	0.01 m
Prism Layer Total Thickness	0.01 m
Maximum Size/Thickness Ratio	10.0
Maximum Cell Size	1.0 m

A custom surface control was used on the rocket fin and body with surface remeshing enabled and a Target Surface Size of 0.005 m. A custom volumetric control was used in a cone shaped region towards the end of the rocket with a custom Isotropic Size of Trimmer Mesh equal to 0.05 m. The mesh of the entire region can be seen in Figure 11, with an XZ plane view of the mesh shown in Figure 12 and the mesh around the fin shown in Figure 13.

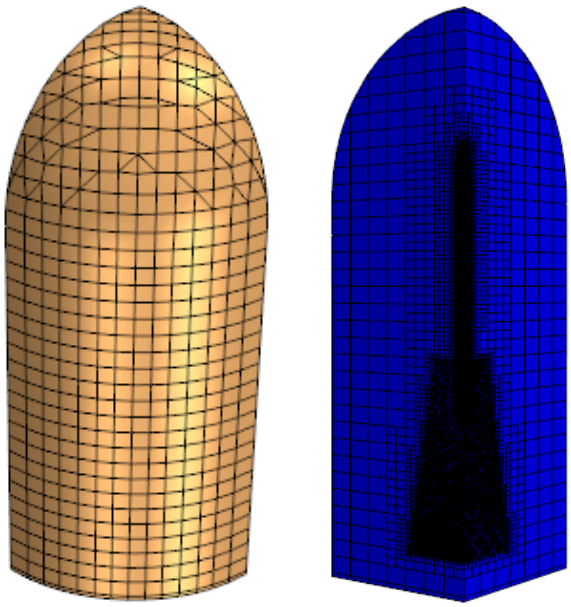

Figure 11: Full region mesh of model.

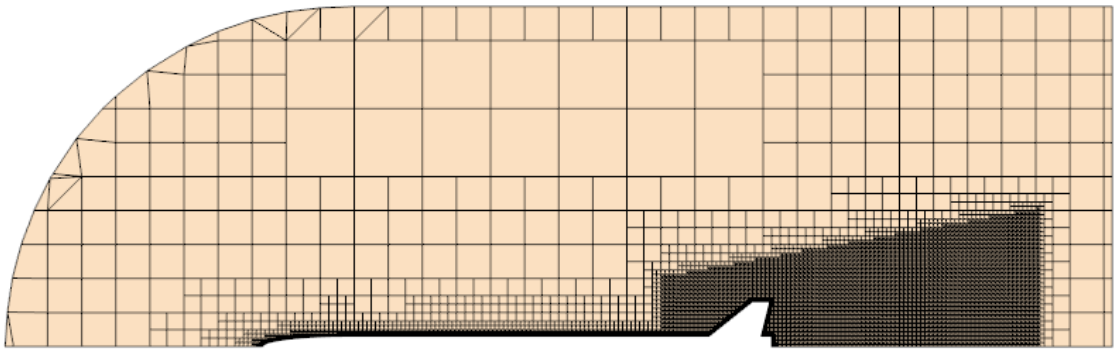

Figure 12: XZ plane view of mesh with cone-shaped volumetric control applied to end of rocket and surface control applied to rocket body and fin.

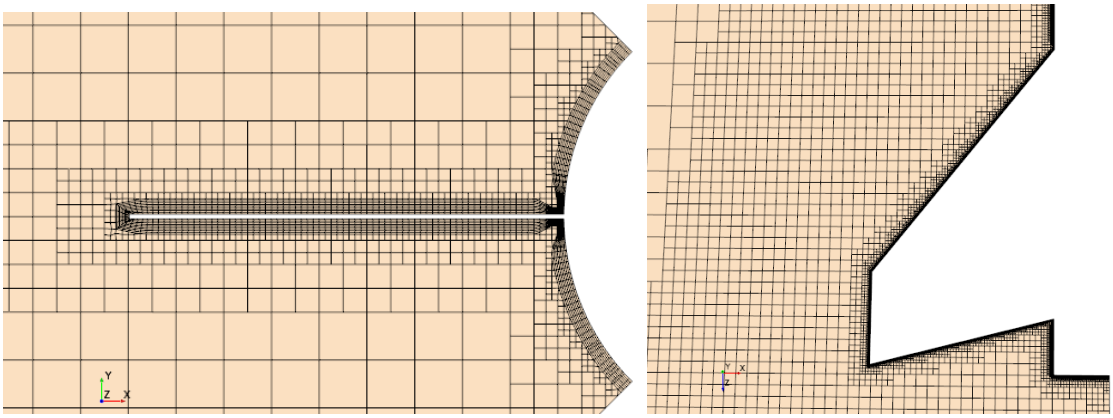

Figure 13 LEFT: XY plane view of mesh around rocket outer diameter and fin showing prism layer and mesh growth. RIGHT: XZ plane view of mesh around fin showing prism layer, mesh growth, and volumetric control region.

5. Results and Discussion

Four runs were attempted on the first model (an RT fin), with varying values for Prism Layer Thickness and Prism Layer Near Wall Thickness. The results of these runs are summarized in Table 6, with convergence reached in Run 4 (using the final values mentioned in Section 4).

Table 6: Results from Prism Layer modifications for each run

Control	Run			
	1	2	3	4
Prism Layer Thickness	0.05	0.025	0.05	0.01
Prism Layer Near Wall Thickness	0.015	0.015	0.01	0.01
Iterations Run	548	169	36	228
Convergence?	No	No	No	Yes
Notes	< 10 cell corrections	Cell corrections on 10 to 20 cells	Cell corrections on < 10 cells	

Convergence was determined by plots of the coefficients of drag and lift on the fins. The convergence plots that coincide with the four runs from Table 6 are shown in Figure 14, with the residuals shown in Figure 15. The residuals do not, however, seem to converge.

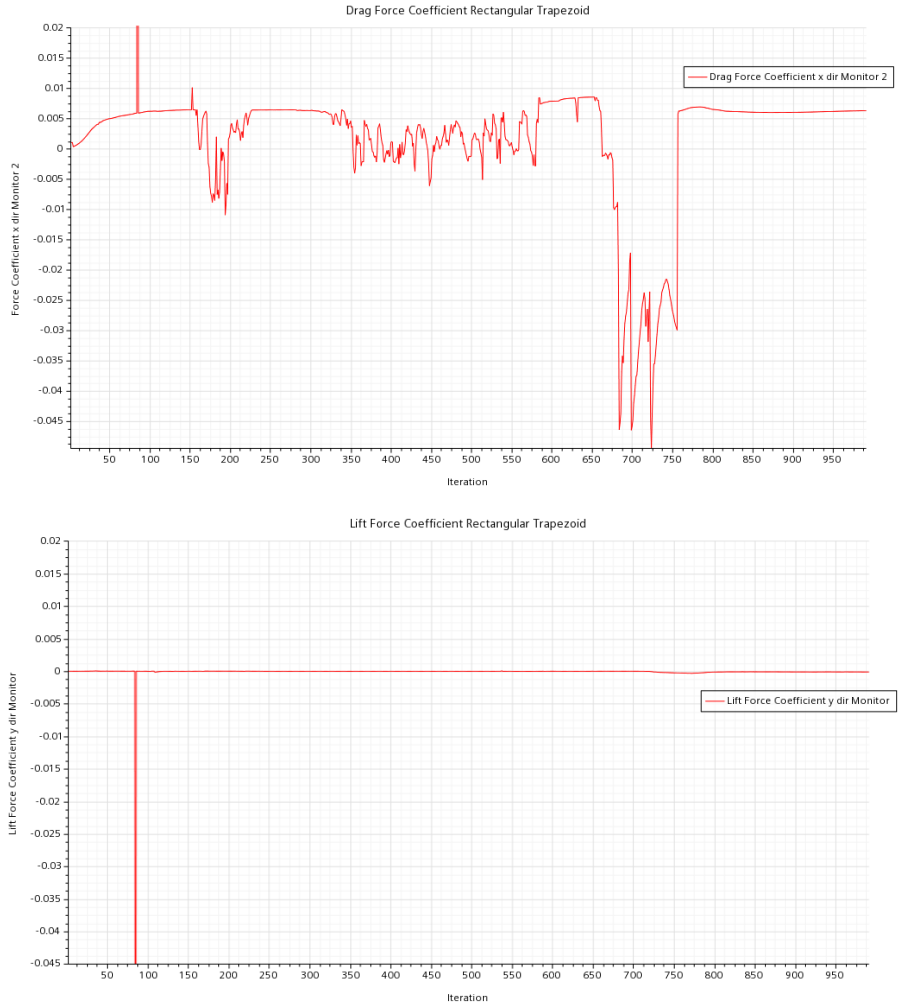

Figure 14: Convergence plots for RT model with four runs of varying mesh parameters mentioned in Table X. TOP: Drag Coefficient. BOTTOM: Lift Coefficient.

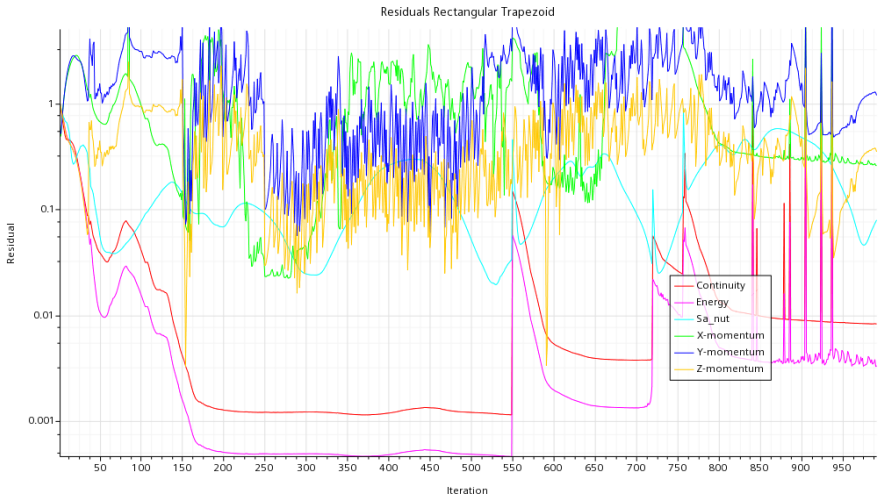

Figure 15: Residuals plot for RT model with four runs of varying mesh parameters mentioned in Table X.

The Mach number scalar scene for RT fins can be seen in Figure 16, with a shock wave occurring behind the body of the rocket. This wave will be affected by the addition of the rocket engine, which protrudes from the end of the rocket, and does not result from the fin geometry. The streamlines for RT and DT fins are compared in Figure 17, with the stagnation point of the rectangular cross section evident in the RT streamlines but reduced in the DT streamlines.

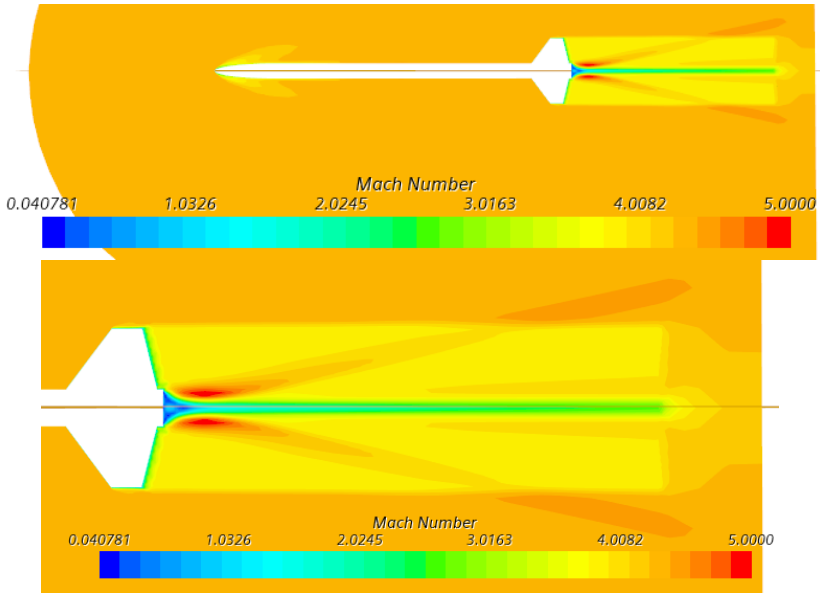

Figure 16: Plane view of Mach Number scene for RT fins, with shock wave shown behind rocket. TOP: Full rocket body. BOTTOM: Close-up of fin can and flow.

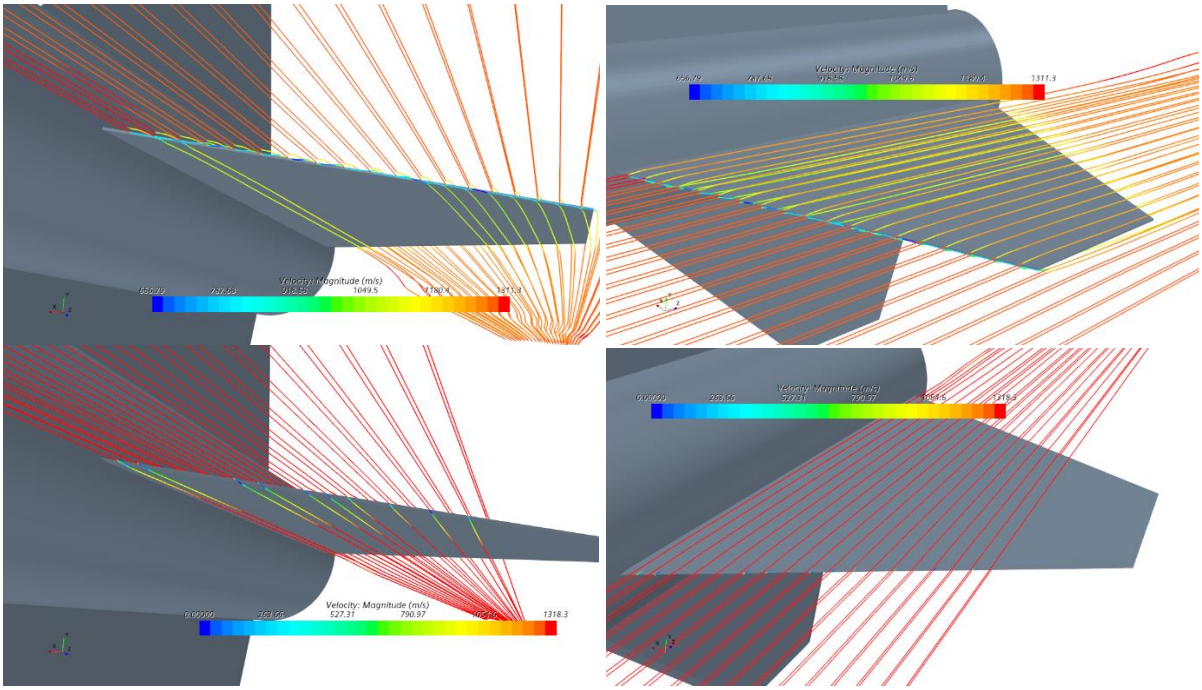

Figure 17: Streamlines around trapezoidal fins as viewed from below (LEFT) and above (RIGHT). TOP: RT fin. BOTTOM: DT fin.

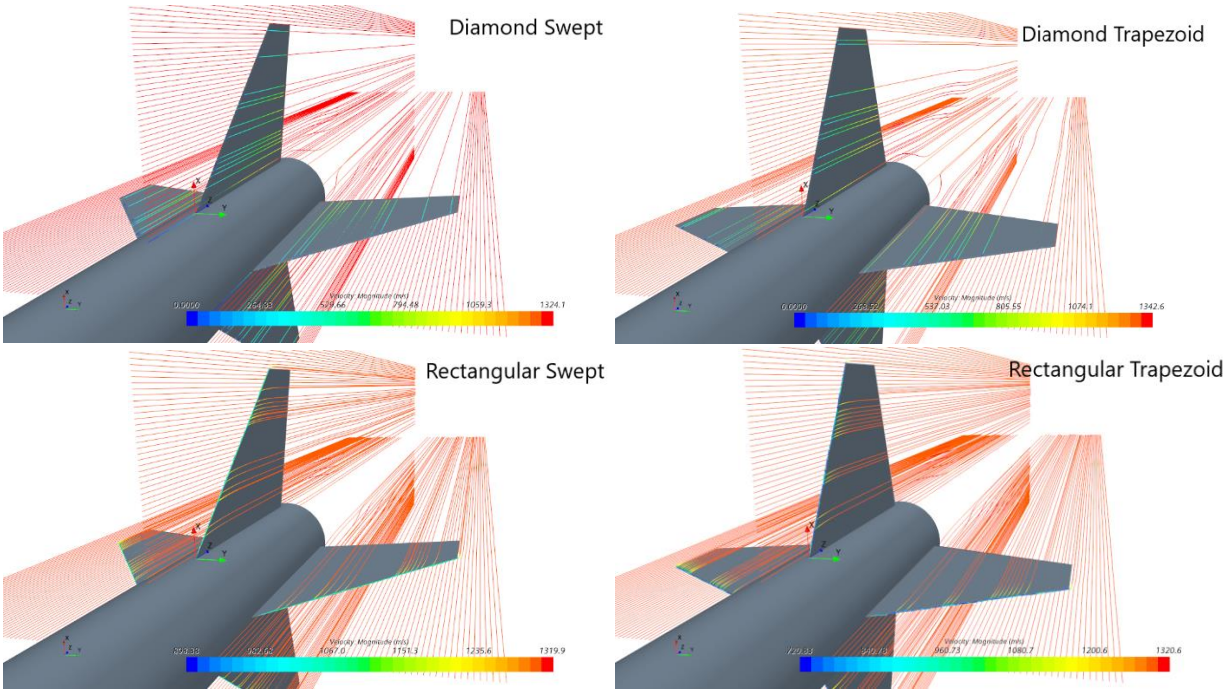

The coefficients of drag (Cd) and lift (Cl) for the four fin shapes were extracted (using the same planform area of 400 in^2 as reference) and are presented in Table 7. Unlike the other shapes, the Cl for the RT fin is not zero as expected. The reason for this is unclear currently but possibly a result of rounding errors. The coefficient of drag is an average 8.6 times higher for a rectangular cross section than a diamond cross section, and an average 1.5 times higher for a trapezoidal fin than a swept fin. However, upon further analysis when writing this report, it was discovered that the boundary surfaces for the diamond cross section fins were created incorrectly, with the chamfered faces joined with the rocket body boundary instead of the fin boundary. This may result in errors and will be corrected in further analysis.

Table 7: Summary of Drag and Lift Coefficients for the four fin shapes.

	Cd	Cl
RT	0.0063	-0.0001
DT	0.0007	0
RS	0.0041	0
DS	0.0005	0

Two line probes were created along the front surface of the fins, one at the base and one at the top, corresponding to the locations of interest seen in the pressure scenes (Figure 18). The pressure at each point along the line probe was plotted, with the results for each fin compared in Figure 19. The swept fins have longer z-distances due to their geometry. As expected, the pressure is higher for rectangular cross sections. However, the error in boundary modeling means that the values of pressure for the diamond cross sections may be incorrect. The RT fin experienced a maximum of 64569 Pa at z = 0.053 in, with the RS fin experiencing a maximum of 34312 Pa at z = 0.476 in, a difference likely due to decrease in slope of the frontal surface on the RS fin. Additionally, the pressure scene in Figure 18 shows a distribution that is not symmetric on the fin. The reason for this is currently unknown.

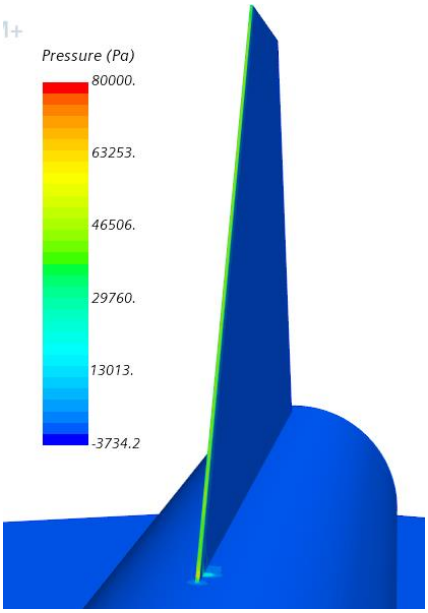

Figure 18: Pressure scalar scene along front surface of RT fin, showing regions of interest at base of fin and top of fin.

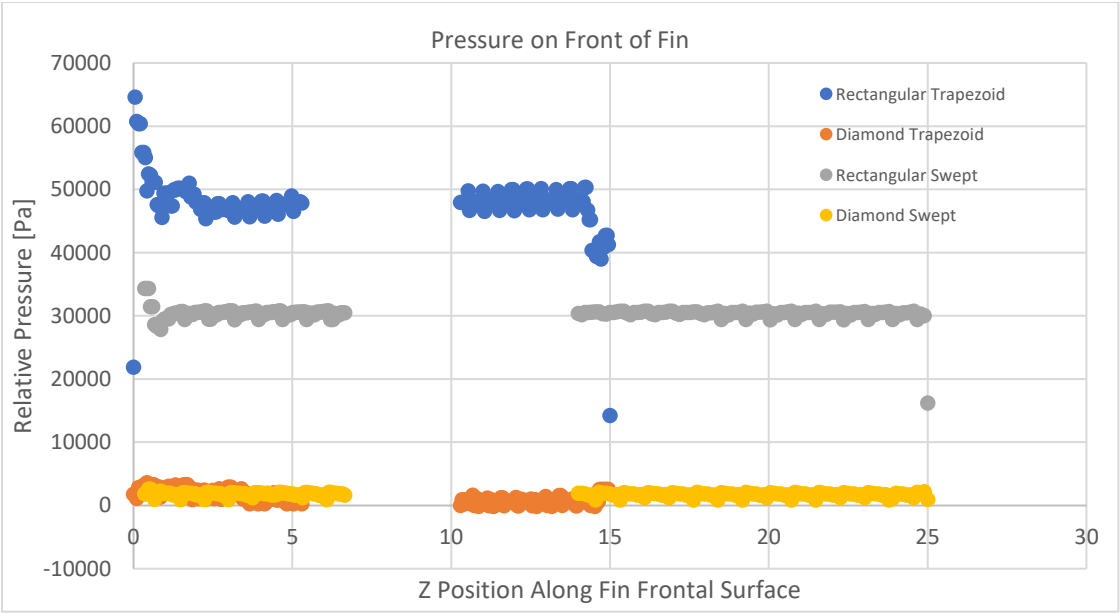

Figure 19: Pressure distribution plot on centerline of frontal surface of fins.

Table 8: Summary of Drag Force and max frontal pressure for the four fin shapes at max dynamic pressure.

	FD (N)	P (psi)
RT	274.67	31
DT	45.89	5.8
RS	132.74	13.8
DS	93.05	6.05

6. Conclusion

The fins with a rectangular cross section experience higher drag forces and higher pressure on their front surfaces than the fins with diamond cross sections. Fins with trapezoidal planform areas also experience higher drag and pressure than fins with swept planform areas. Thus, the optimal fin shape to reduce drag and pressure would be a swept fin with a diamond cross section.

Future work for this project includes:

- Properly defining the diamond cross section fins boundary surfaces and re-running the simulations
- Varying the dimensions of the four fin shapes
- Investigating reason for RT coefficient of lift being non-zero
- Investigating reason for pressure distribution being non-symmetric on fin surface
- Comparing Mach number scenes and streamlines for all four fin shapes
- Comparing coefficients of drag and lift for varying angles of attack

In this project I learned about: modeling supersonic flow physics at high altitudes; generating a refined surface mesh to create proper geometry; how the prism layer properties affect convergence for a turbulent flow; investigating drag, lift, and pressure on a fin/airfoil; and visualizing the Mach number, streamlines, and pressure scenes of an axisymmetric model projected to a full model.

7. References

[1] “LV4 MDO Simulation and Optimization,” Portland State Aerospace Society, retrieved February 2021. https://github.com/psas/lv4-mdo/tree/master/Simulation_and_Optimization

[2] Ewing, P., “Best Practices for Aerospace Aerodynamics,” *STAR South East Asian Conference*, Singapore, June 2015. http://mdx2.plm.automation.siemens.com/sites/default/files/Presentation/ExternalAero_SEA-ugm-2015.pdf

[3] “Transonic Flow: RAE2822 Airfoil,” STAR-CCM+ User Guide, Siemens, retrieved March 2021.